Self-Contained Frequency Trimming of Micromachined Silicon Resonators via Localized Thermal Oxidation

Arash Hajjam and Siavash Pourkamali, *Member, IEEE*

***Abstract*—An electronically controllable frequency trimming technique based on localized thermal oxidation of single crystalline silicon resonators is demonstrated. Thin layers of silicon dioxide can be thermally grown on silicon surfaces of resonant structures via extreme joule heating of such when biased with relatively large bias currents in an oxygen-rich environment. Changes in structural stiffness or oxidation induced internal stress causes a shift in the resonant frequency of the structures that can be used for post-fabrication frequency trimming of silicon resonators. As an added advantage, the positive temperature coefficient of Young's modulus for the added silicon dioxide layer can partially compensate the large negative temperature coefficient of frequency (TCF) for the silicon resonators. Frequency trimming as high as ∼3.7% and TCF as low as 0.2 ppm/°C has been demonstrated for a 54 MHz I-shaped resonator using this technique. Furthermore, it has been demonstrated that coupling of mechanical resonance to electrical resistance and consequently joule heating of the structure can lead to a cooling effect at mechanical resonant frequency of the structure that allows the localized oxidation to stop automatically as soon as the resonator frequency reaches a targeted actuation frequency applied to the structure. The viability of this concept is demonstrated by application of both off-resonance and at-resonance actuation signals to fabricated resonators showing that as opposed to the off-resonance signals, the at-resonance signals with the same intensity do not lead to further frequency shift. [2012-0337]**

***Index Terms*—MEMS resonator, frequency trimming, thermal actuation, micro-resonator, piezoresistive readout, temperature compensation, localized oxidation**

I. Introduction

MICRO-ELECTRO-MECHANICAL resonators are of great interest for miniaturized highly stable frequency generation as well as resonant mass sensing for molecular or particulate detection [1]–[5]. Resonance frequency of micromechanical resonators is dependent on the physical dimensions of the resonating structure. Even very small (few nanometers) fabrication induced dimensional imprecision can lead to intolerable frequency inaccuracies for micromechanical resonators. Therefore, process variations across the substrate (e.g. non-uniformities in photolithography, etching and film thickness) leading to variations and mismatch in the mechanical resonant frequencies are a major challenge for batch fabrication of micromechanical resonators [1], [3]. Achieving ppm level frequency accuracy and uniformity in batches of micromachined resonators is a challenging task necessitating post-fabrication trimming [6].

Frequency trimming techniques for silicon based micromechanical resonators include pulsed-laser-removal/trimming, electrostatic trimming and other process alterations. Post-fabrication frequency trimming via pulsed-laser-removal/deposition [6], [7] is shown to be a method that provides ppm level frequency. Other than that, digital trimming techniques use a high resolution fractional-N synthesizer in a phase lock loop architecture for locking a voltage-controlled oscillator to a silicon microresonator-based reference oscillator [6]. Such techniques are however power hungry and considerably increase the overall phase noise of the oscillator and the integrated circuit die area.

Other post fabrication processes such as gold diffusion into the bulk of the resonator have also been demonstrated for frequency trimming purposes. In this method by running a current through the structure, it is heated up resulting in a gold coating to diffuse into the resonator silicon structure. Upon cooling, the gold diffusion slightly increases the stiffness of the resonating structure, which results in an upward shift in resonance frequency [8]. This technique requires additional process steps to add the gold layer. Furthermore, the residual gold film on the device surface can deteriorate device performance and quality factor. Also, none of the other techniques mentioned have the ability to provide self-controlled simultaneous tuning of multiple devices.

In this paper a relatively simple technique for electronically controlled post-fabrication frequency trimming of individual silicon resonators is presented. This approach is based on passing a large current through the structures locally raising their temperature to several hundred degrees Celsius, which enables thermal oxidation of the silicon surfaces when placed in an oxygen rich atmosphere. A number of factors including the change in dimensions and effective Young's modulus as well as oxidation induced internal stress cause a change in the resonance frequency of the silicon resonator. The effect of change in Young's modulus and dimensions

Manuscript received November 20, 2012; revised March 10, 2013; accepted May 11, 2013. Date of publication June 11, 2013; date of current version September 27, 2013. Subject Editor C. Nguyen.

A. Hajjam is with the Department of Electrical and Computer Engineering, University of Denver, Denver, CO 80208 USA (e-mail: ahajjam@du.edu).

S. Pourkamali is with the Department of Electrical Engineering, University of Texas at Dallas, Richardson, TX 75080 USA (e-mail: siavash.pourkamali@utdallas.edu).

Color versions of one or more of the figures in this paper are available online at http://ieeexplore.ieee.org.

Digital Object Identifier 10.1109/JMEMS.2013.2263218

almost cancel each other out, making the relatively hard to predict effect of stress more pronounced. For this reason, different devices behave differently depending on their exact topology, dimension, and oxidation conditions. Therefore a permanent change in the resonant frequency of the device can be seen in either the upper or lower direction. In the latter part of the paper the potential for self-contained implementation of the same technique for automated batch frequency trimming is discussed and demonstrated. Coupling of the piezoresistivity of the structural material with mechanical resonance can lead to reduction of joules heating generated by an AC excitation in a resonating structure. This can lower the temperature and stop the localized oxidation process as soon as mechanical vibrations start due to the trimmed mechanical resonant frequency reaching the target excitation frequency.

II. Resonator Description and Fabrication

The resonators utilized in this work are referred to as I-shaped Bulk Acoustic Resonators (also known as dog-bone resonators) [9,10]. The schematic view of an I-shaped resonator is shown in Figure 1a. Although thermal actuation along with piezoresistive sensing has been used in this work for operation of the devices, the same trimming techniques can be applied to similarly structured resonators with electrostatic, piezoelectric or other transduction mechanisms. Thermal actuation occurs by passing a fluctuating electrical current through the actuator beams in the middle of the structure. The operating principle of thermally actuated resonators has thoroughly been explained in [9].

Figure 1b shows the qualitative temperature distribution of an I-shaped resonator while passing a DC current through the structure. Due to the effects of heat convection, the plates have a lower static temperature than the narrower sections of the structure where both ohmic heat generation and thermal resistance are maximized. Therefore, when exposed to an oxygen rich atmosphere, silicon dioxide will be formed on the hot surfaces of the structures in the middle of the structure when heated to high enough temperatures.

The standard single mask SOI MEMS process was used for fabrication of the suspended resonant structures. This process includes carving the single crystalline silicon structures into the SOI device layer using deep reactive ion etching followed by removing the underlying buried oxide layer (BOX) in hydrofluoric acid (HF) [9].

Figure 2 shows the SEM view of a fabricated 53 MHz IBAR. The resonator was fabricated on a low resistivity N-type SOI substrate with buried oxide (BOX) thickness of 5 μm.

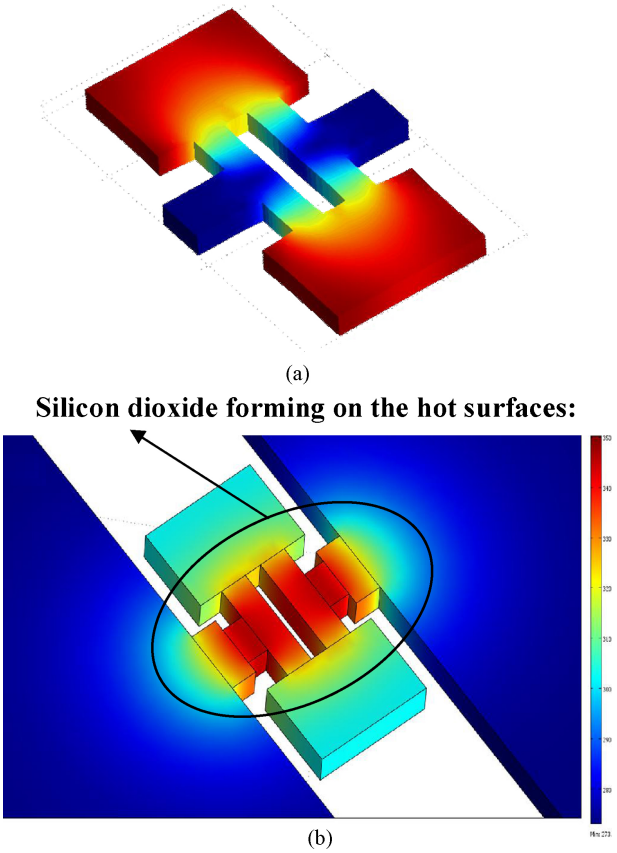

Fig. 1. a) COMSOL modal analysis, showing the fundamental in-plane resonance mode shape for an I-shaped resonator. In this work thermal actuation was used for operation of the devices. Red and blue colors show locations with the largest and smallest vibration amplitudes respectively. b) Schematic view of an I-shaped resonator biased with a DC current. The bias current passes through the structure heating it up by the resulting ohmic loss.

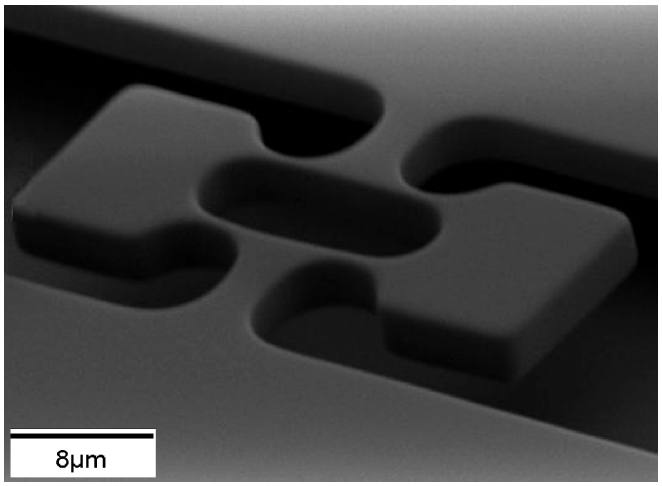

Fig. 2. SEM view of a 53 MHz I-shaped resonator. The resonator is fabricated on a low resistivity (~0.01 Ω.cm) N-type SOI substrate using a single mask process.

III. Frequency Trimming Setup

Figure 3 shows the schematic diagram of the test setup used for performing the localized thermal oxidation process. The silicon chip containing the resonators was first placed on a printed circuit board (PCB) containing coaxial connections to the measurement equipment. The PCB was then placed in a custom made plastic chamber while connected to the measurement setup using electrical feedthroughs. In this setup, oxygen from a pressurized tank was bubbled through a heated water container to absorb moisture and was then delivered into the chamber that the resonator samples were located inside of. Moisture was added to oxygen in order to provide a suitable atmosphere for wet oxidation of silicon and

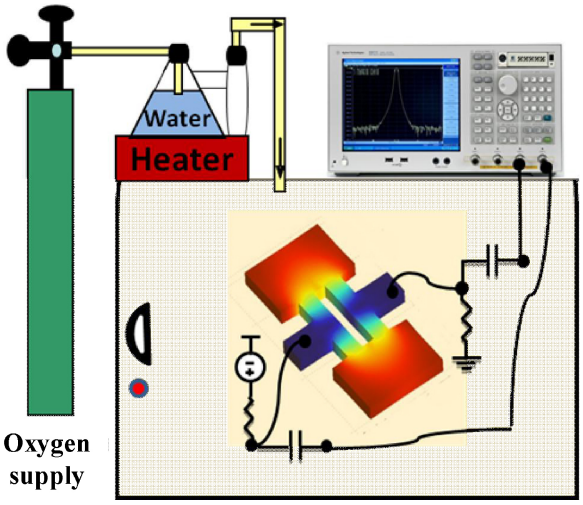

Fig. 3. Schematic diagram of the measurement setup used in this experiment. Moisture rich oxygen was driven into the chamber while the device was biased at a high current (the beams were red). Real time resonant frequency measurements were performed by a network analyzer.

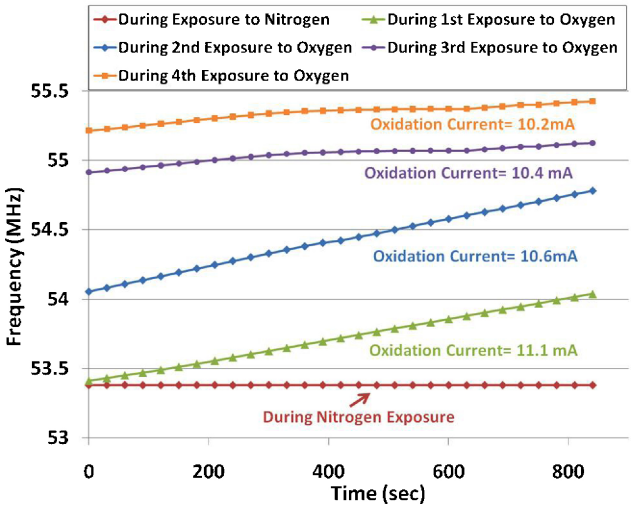

Fig. 4. Change in the measured resonance frequency for the 53 MHz resonator as a function of the exposure time during 4 oxidation steps showing an overall frequency shift of ~2 MHz. No frequency shift was recorded when the resonator was exposed to nitrogen.

hence significantly increase the reaction rate (reduce reaction time) compared to dry oxygen.

The localized oxidation and therefore frequency trimming starts by application of a relatively large bias current, more than what is typically required for operation of the device. Assuming the resonator resistance being ~150 Ω, at a current range of 1-5 mA, a power range of 150mw to 750mW is expected. At that power, the actuator beams visibly turn red on the silicon substrate). The heating of the actuator beams together with the provided humid atmosphere inside the chamber, enables oxidation to occur on the surface of the beams. The forming of the oxidation on the surface of the beams is responsible for both the frequency trimming and temperature compensation of the resonators.

A more advanced version of the localized oxidation based trimming approach was later carried out for which it shows the potential for automation (self-containment) of this technique. In this self-contained trimming approach, instead of utilizing a DC current for localized heating of the device instead an AC current enough to provide the heating required for oxidation of the resonators was applied across the beam structure.

IV. Measurement Results

Figure 4 shows the change in the measured resonance frequency for the 53 MHz resonator of Fig. 2 over time, during 4 oxidation steps. As the oxidation process starts, the internal stress of the thermal actuators changes. This causes the resonance frequency of the resonator to gradually change. An overall frequency shift of ~2 MHz was observed. As can be seen in Fig. 4, the slope of the changes decrease in the last steps. This expected decrease is due to the nature of the oxidation process that slows down as the oxide thickness increases. In order to confirm that the change in frequency is caused by thermal oxidation of the resonator, the same self heating procedure was also performed in a nitrogen atmosphere. This time, no frequency shift was observed and the frequency of the resonator remained constant throughout the whole process.

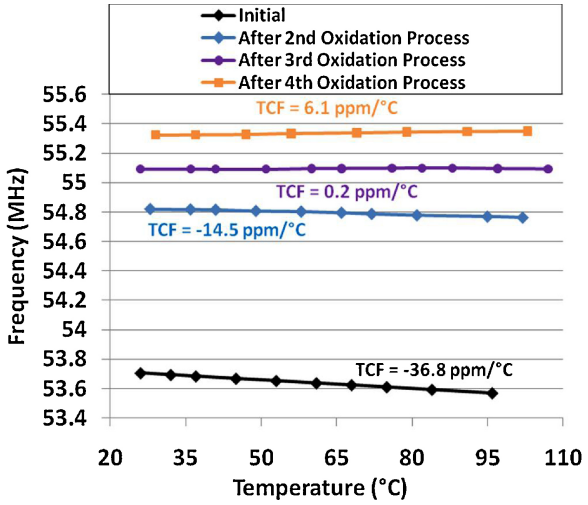

Fig. 5. Temperature drift characteristics for the 53 MHz resonator of Fig. 2 measured before and after each of the oxidation steps. The TCF value becomes more positive (less negative) after each step due to the formation and thickening of SiO_2 on the surface of the actuators.

Another set of interesting data that was collected was with regard to the resonator temperature drift. Figure 5 shows the temperature drift characteristics of the same resonator measured before and after each of the oxidation steps. Silicon resonators typically exhibit temperature coefficient of frequency (TCF) in the -20 to -40 ppm/°C range [10], [11]. Figure 5 shows that while the initial TCF for this resonator was measured to be -37 ppm/°C, its value has gradually increased (become less negative) after each oxidation step. After the third oxidation step, the TCF value turns positive (0.2 ppm/°C) and even becomes substantially positive (6.1 ppm/°C) after the forth oxidation step. This increase in TCF is due to the formation and thickening of the SiO_2 film (which has a positive

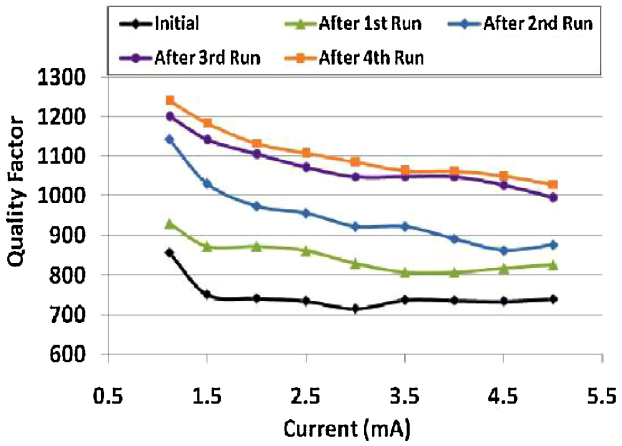

Fig. 6. Measured quality factor for the 53 MHz resonator at different bias currents after each oxidation step. The quality factor has slightly increased after each step.

temperature coefficient of Young's modulus) on the surface of the resonator [12]. Thus, the potential of achieving highly suppressed temperature drifts through the same technique is also demonstrated.

Figure 6 depicts the measured quality factors of the 53 MHz resonator at different bias currents. This frequency trimming process is a relatively intense treatment of the resonators and it was thought that it could cause structural damage to the device. Therefore the measured Q values were monitored to see if this really is the case. The results showed that after each oxidation step, the quality factor has not only not degraded, but slightly increased. Therefore using this trimming technique, the variations in the resonator microfabrication processes have been compensated without compromising the performance of such.

A. Self-Contained Trimming Principle

As opposed to the experiment presented in the previous section in which a DC current was used for localized heating of the device, an AC voltage ($V_{ac}\cos(2\pi f_a t)$) (Figure 7a) applied across the structure can provide the heating required for localized thermal oxidation. The generated power has a square relationship with the applied voltage and gives birth to two frequency components at DC and twice the actuation frequency ($2f_a$):

$$P = \frac{v_{ac}^2 \cos^2(2\pi f_a t)}{R_A} = \frac{v_{ac}^2}{2R_A} + \frac{v_{ac}^2 \cos(4\pi f_a t)}{2R_A} \qquad (1)$$

where R_A is the electrical resistance of the resonator and f_a is the actuation frequency. The DC power component translates to a static elevated temperature of the thermal actuators, while the AC component leads to small temperature fluctuations at twice the actuation frequency. It can be shown that the AC temperature term is proportional but also has a 90° lag in comparison to the AC power due to the thermal time constant of the structure being much larger than $1/4\pi f_a$. [13]. The resulting fluctuating temperature causes a thermal stress and therefore an alternating mechanical force inside the thermal actuators. If the resulting applied force has the same frequency

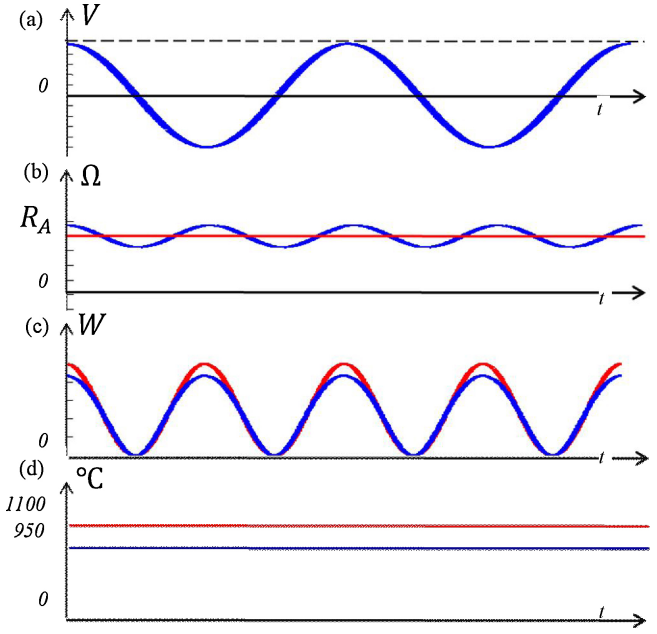

Fig. 7. Waveform representation of a) Input AC voltage, b) Resistance of the resonator, c) Ohmic loss and d) Temperature in both conditions of off-resonance (red) and at-resonance (blue). It is assumed that $r_{ac} = 0.15R_A$. Therefore, the DC power consumption drops 14% during resonance with respect to its off-resonance mode. As a result assuming the initial static temperature of 1100 °C, temperature decreases to 950 °C.

as the resonance frequency of the resonator, it can excite its vibration mode. In order for this to happen, the frequency of the actuation voltage should be half of the mechanical resonant frequency. Due to the mechanical lag in damped mass-spring systems, the resulting mechanical vibration of the resonator has a 90° lag with respect to the mechanical force [13]. The mechanical vibration leads to resistance fluctuations of the resonator due to the piezoresistive effect. The resistance fluctuations are proportional and in phase with the mechanical vibration. Therefore, the resulting resistance fluctuations added to the stationary electrical resistance of the device has an overall lag of 180° with respect to the applied actuation current due to thermal and mechanical delays. For N-type silicon the piezoresistive coefficient is negative which itself adds a 180° phase shift. Thus, the resistance fluctuation will be in phase with the applied voltage (blue plot in Figure 7b) and this leads to the overall resistance of: $R_A + r_{ac}\cos(2\pi f_0 t)$. As a result the ohmic power in the structure will be:

$$P = \frac{v_{ac}^2 \cos^2(\pi f_0 t)}{R_A + r_{ac}\cos(2\pi f_0 t)} = \frac{v_{ac}^2 (1 + \cos(2\pi f_0 t))}{2(R_A + r_{ac}\cos(2\pi f_0 t))}. \qquad (2)$$

The r_{ac} value itself is equal to:

$$r_{ac} = \frac{R_A |\pi_l| E x_m}{L} \qquad (3)$$

where π_l is the longitudinal piezoresistive coefficient, E is the young's modules, L is the length of the thermal actuator and x_m is the vibration amplitude. The DC component of Eq.2 can be approximately found to be equal to:

$$P_{DC} \cong \frac{v_{ac}^2}{2(R_A + r_{ac})} \qquad (4)$$

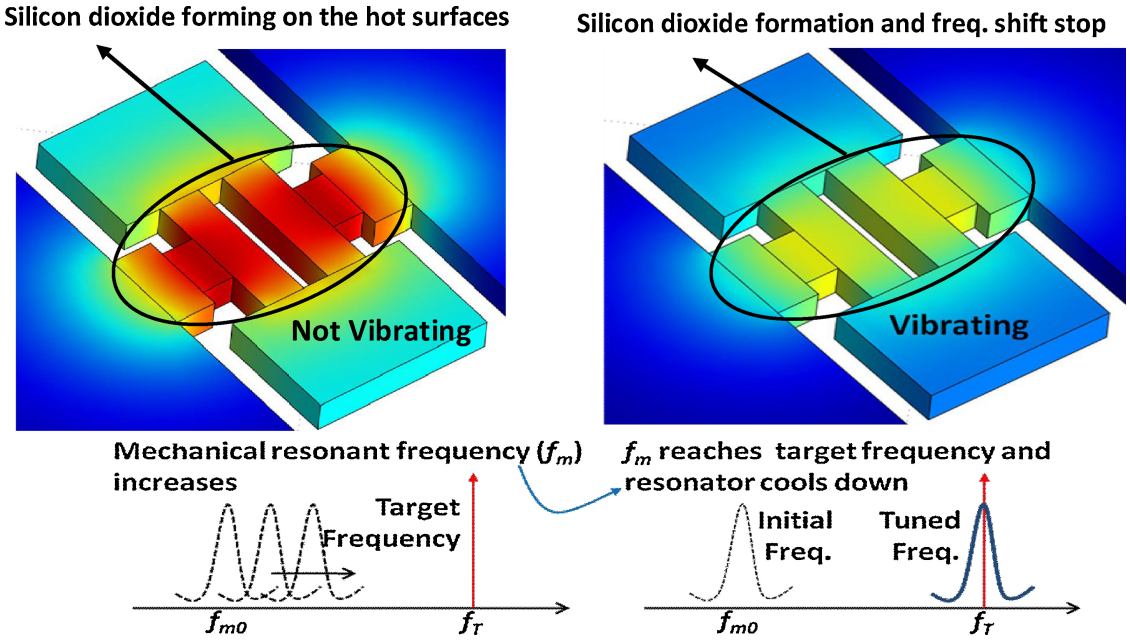

Fig. 8. Schematic demo of the frequency trimming technique. When an actuation voltage with half the target resonance frequency is being applied across the actuator beams, the elevated temperature allows oxidation to take place on their surface. As a result, the structural stiffness gradually changes and the resonant frequency moves toward the target. When the mechanical resonant frequency reaches the target frequency, the resonator starts vibrating and therefore cools down. As a result, oxidation stops and the frequency will not shift further.

By comparing the DC power consumptions in the two different states of off-resonance (DC component of Eq. 1) and at-resonance (Eq. 4), it is obvious that at-resonance state the static ohmic power generation decreases (Figure 7c).

In conclusion, if the applied AC actuation voltage has the right frequency to excite vibration mode of the resonator, its resulting static joule heating will be smaller compared to an actuation voltage with the same amplitude but different frequency (Figure 7d). The difference in temperature between the two cases of at-resonance and off-resonance can be utilized for self-contained trimming of the structures. With relatively large vibration amplitudes and large piezoresistive coefficients, r_{ac} can become comparable with $R_{DC.}$ For instance, with a conservative piezoresistive coefficient of $(-10 \times 10^{-11}\text{Pa}^{-1})$, and vibration amplitude of 100x smaller than the actuator length, $r_{ac} = -0.15R_A$. In this case the value of P_{DC} at resonance becomes 14% less than its value out of resonance. This translates to a 14% reduction of the actuator static temperature difference from the surroundings. For instance, a resonator heated up to 1100 °C by the applied currents out of its resonance frequency, can cool down to about 950 °C if the actuation frequency becomes equal to its mechanical resonant frequency. Sharp dependence of thermal oxidation rate on temperature can turn small temperatures changes into major changes in the oxidation rate and even completely stopping it.

Figure 8 schematically depicts the envisioned self-contained electronic frequency trimming technique for micromechanical single crystalline silicon resonators. Assuming that a fabricated resonator has resonant frequency of f_{m0} that is slightly different from the desired target frequency (f_T), AC actuation voltage at half the desired frequency is to be applied to the resonator. To initiate the frequency trimming process, amplitude of the actuation voltage should be sufficient to elevate the temperature of the narrow parts of the structure to temperatures required for thermal oxidation. The oxidation process goes on until the resonance frequency of the resonator exactly matches the desired resonance frequency. At this point, the resonator starts vibrating and therefore the overall resonator static temperature drops significantly which could stop the local oxidation. In this manner, the resonant frequencies of a large number of fabricated resonators can be trimmed to a single desired value simultaneously by applying the same actuation voltage to all of them and without the need for individual monitoring and control.

B. Self-Trimming Measurement Setup and Results

In order to perform the localized thermal oxidation process, the same setup shown in the previous part was used but instead of a DC heating current, a large amplitude AC signal was applied through the structure using a function generator.

After each AC actuation induced localized oxidation step for 800 seconds, the devices were disconnected from the AC voltage source and were tested at room temperature using a network analyzer.

Figure 9 shows the change in the measured resonance frequency after different oxidation steps, for an 18 MHz resonator. Different plots show data taken after localized oxidation runs via actuation by AC voltage with both off-resonance and at-resonance frequencies. It has been shown through 4 consecutive oxidation periods with alternating off/at resonance signals applied to the device, that the cooling effect is occurring. Off-resonance oxidation which has been applied in steps 1 and 3 has led to changes in the resonator

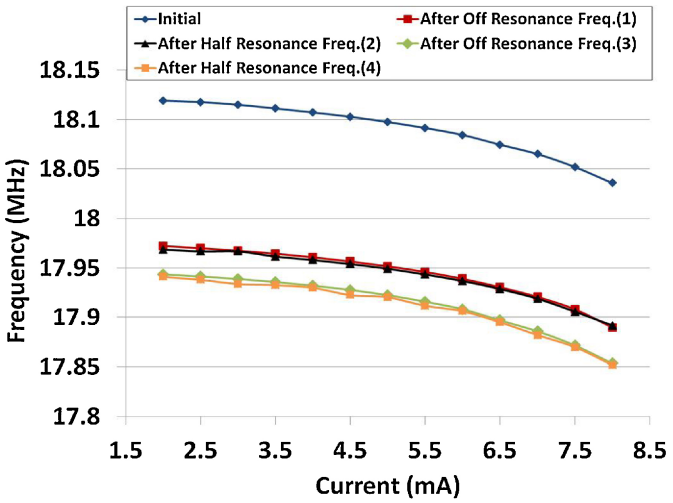

Fig. 9. Measured resonance frequency of the 18 MHz resonator, at different bias currents. Different plots show the data taken after different localized oxidation runs at room temperature when the oxygen source was removed. As can be seen from the graph, the actuation at half the resonance frequency has had no effect on the shift in resonant frequency (steps 2 and 4), whereas each time the resonator was actuated at an off-resonance frequency, the resonance frequency has decreased.

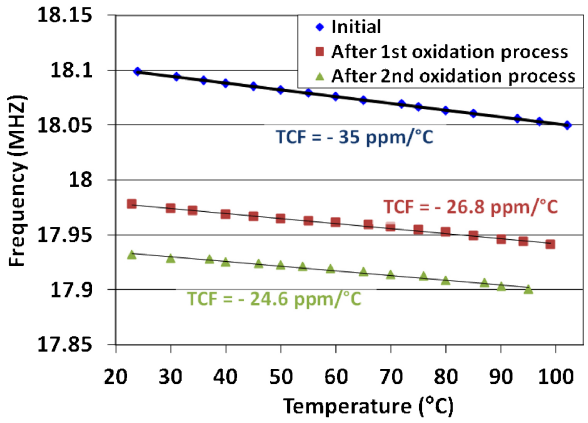

Fig. 10. Temperature drift characteristics for an 18 MHz resonator measured before and after each of the oxidation steps. The TCF becomes more positive (less negative) after each off-resonance actuation step due to the formation and thickening of SiO_2 on the surface of the actuators.

frequency, whereas in steps 2 and 4 it is shown that when the excitation causes mechanical resonance, it results in almost no oxidation (no frequency trimming). In order to find the frequency at which the mechanical resonance is caused, the power was calculated at both DC and AC modes and they were set to equal values and then the right frequency value was derived.

Figure 10 shows the temperature drift characteristics of the same resonator measured before and after each of the oxidation steps. It shows that while the initial TCF for this resonator was measured to be -35 ppm/°C, its value has gradually increased (become less negative) after oxidation steps with off resonance frequency. Due to no oxidation occurring when mechanical at-resonance actuation voltage is applied, no change in TCF is expected.

V. Conclusion

Post-fabrication trimming of I-shaped single crystalline silicon thermal-piezoresistive resonators, via localized self-induced thermal oxidation was demonstrated. The presented post fabrication trimming technique offers the possibility to precisely compensate for variations in the resonator microfabrication processes without compromising the performance of such. Temperature compensation was also achieved due the formation of silicon dioxide films on the surface of resonator actuator beams.

Furthermore, self-contained post-fabrication electronic frequency trimming of individual single crystalline silicon resonators was demonstrated. Self-containment can be achieved by taking advantage of the cooling effect of resonators at resonance. This technique can potentially be used for automated simultaneous trimming of a whole batch of resonators after fabrication.

References

[1] R. Abdolvand, H. Mirilavasani, G. K. Ho, and F. Ayazi, "Thin-film piezoelectric-on-silicon resonators for high-frequency reference oscillator applications," *IEEE Trans. Ultrason. Ferroelectr. Freq. Control*, vol. 55, no. 12, pp. 2596–2606, Dec. 2008.

[2] C. T.-C. Nguyen, "MEMS technology for timing and frequency control," *IEEE Trans. Ultrason. Ferroelectr. Freq. Control*, vol. 54, no. 2, pp. 251–270, Feb. 2007.

[3] A. Hajjam, J. C. Wilson, A. Rahafrooz, and S. Pourkamali, "Fabrication and characterization of thermally actuated micromechanical resonators for airborne particle mass sensing: II. Device fabrication and characterization," *J. Micromech. Microeng.*, vol. 20, no. 12, p. 12501, Dec. 2010.

[4] M. Rinaldi, C. Zuniga, C. Zuo, and G. Piazza, "Super-high-frequency two-port AlN contour-mode resonators for RF applications," *IEEE Trans. Ultrason. Ferroelectr. Freq. Control*, vol. 57, no. 1, pp. 38–45, Jan. 2010.

[5] A. Hajjam and S. Pourkamali, "Fabrication and characterization of MEMS-based resonant organic gas sensors," *IEEE Sensors J.*, vol. 12, no. 6, pp. 1958–1964, Jun. 2012.

[6] W.-T. Hsu and A. R. Brown, "Frequency trimming of MEMS resonator oscillators," in *Proc. IEEE Int. Freq. Control Symp.*, 2007, pp. 1088–1091.

[7] M. A. Abdelmoneum, M. U. Demirci, S. S. Li, and C. T.-C Nguyen, "Post-fabrication laser trimming of micromechanical filters," in *Proc. IEEE Int. Electron Devices Tech. Dig.*, 2004, pp. 39–42.

[8] A. K. Samarao and F. Ayazi, "Post-fabrication electrical trimming of silicon bulk acoustic resonators using joule heating," in *Proc. IEEE MEMS Conf.*, Jan. 2009, pp. 892–895.

[9] A. Hasjjam, J. C. Wilson, and S. Pourkamali, "Individual air-borne particle mass measurement using high frequency micromechanical resonators," *IEEE Sensors J.*, vol. 11, no. 11, pp. 2883–2890, Nov. 2011.

[10] A. Hajjam, A. Logan, and S. Pourkamali, "Doping induced temperature compensation of thermally actuated high frequency silicon micromechanical resonators," *J. Microelectromech. Syst.*, vol. 21, no. 3, pp. 681–687, Jun. 2012.

[11] K. Sundaresan, G. K. Ho, S. Pourkamali, and F. Ayazi, "Electronically temperature compensated silicon bulk acoustic resonator reference oscillator," *IEEE J. Solid State Circuits*, vol. 42, no. 6, pp. 1425–1434, Jun. 2007.

[12] R. Melamud, S. A. Chandorkar, K. Bongsang, K. L. Hyung, J. C. Salvia, G. Bahl, M. A. Hopcroft, and T. W. Kenny, "Temperature-insensitive composite micromechanical resonators," *J. Microelectromech. Syst.*, vol. 18, no. 6, pp. 1409–1419, Dec. 2009.

[13] A. Rahafrooz, A. Hajjam, B. Tousifar, and S. Pourkamali, "Thermal actuation, a suitable mechanism for high frequency electromechanical resonators," in *Proc. IEEE MEMS*, Jan. 2010, pp. 200–203.

[14] S. Pourkamali, G. K. Ho, and F. Ayazi, "Low-impedance VHF and UHF capacitive SiBARs–Part I: Concept and fabrication," *IEEE Trans. Electron Devices*, vol. 54, no. 8, pp. 2017–2023, Aug. 2007.

Arash Hajjam was born in Tehran, Iran. He received the B.S. degree in electrical engineering from the University of Tehran, Tehran, Iran, in 2005, the M.S. degree in bio-electrical engineering from the Iran University of Science and Technology, Tehran, in 2008, and the Ph.D. degree in the field of electrical engineering from the University of Denver, Denver, CO, USA, in 2012. He is currently a full-time Lecturer and a Sr. Research Scientist at the Department of Electrical and Computer Engineering, University of Denver. He has been an author of over 30 peer-reviewed international journal and conference papers. He is an international patent holder. His current research interests include integrated silicon-based MEMS and microsystems. He was a recipient of the 2012 Best Research Assistant Award and the 2009 Best Teaching Assistant Award at the School of Engineering and Computer Science, University of Denver. He was the recipient of the 2012 Graduate Studies Dissertation Fellowship Award for outstanding research at the University of Denver, and the 2004 Best Student Paper Award at the ISCEE 2004 Electrical Engineering Conference. He is a licensed Professional Engineer (P.E.) in the state of Colorado.

Siavash Pourkamali (S'02–M'06) received the B.S. degree in electrical engineering from the Sharif University of Technology, Tehran, Iran, in 2001, and the M.S. and PhD. degrees in electrical engineering from the Georgia Institute of Technology, Atlanta, GA, USA, in 2004 and 2006, respectively.

From 2006 to 2012, he was an Assistant Professor of Electrical and Computer Engineering at the University of Denver, Denver, CO, USA. He is currently an Associate Professor with the Department of Electrical Engineering, University of Texas at Dallas, Richardson, TX, USA. He holds several issued patents and pending patent applications in the areas of silicon micro/nanomechanical resonators and filters and nanofabrication technologies, some of which have been licensed to major players in the semiconductor industry. His current research interests include integrated silicon-based MEMS and microsystems, micromachining technologies, RF MEMS resonators and filters, and nanomechanical resonant sensors.

Dr. Pourkamali is a recipient of the 2011 NSF CAREER Award, the 2008 University of Denver Best Junior Scholar Award, and the 2006 Georgia Tech Electrical and Computer Engineering Research Excellence Award. He was also a silver medal winner in the 29th International Chemistry Olympiad in 1997.